Preclinical Development of CD38-Targeted [^{89}Zr]Zr-DFO-Daratumumab for Imaging Multiple Myeloma

Anchal Ghai[1], Dolonchampa Maji[1,2], Nicholas Cho[1,2], Chantiya Chanswangphuwana[3], Michael Rettig[3], Duanwen Shen[1], John DiPersio[3], Walter Akers[4], Farrokh Dehdashti[1], Samuel Achilefu[1,2,5], Ravi Vij[3], and Monica Shokeen[1,2]

[1]Department of Radiology, Washington University School of Medicine, St. Louis, Missouri; [2]Department of Biomedical Engineering, Washington University in St. Louis, St. Louis, Missouri; [3]Department of Medicine, Washington University School of Medicine, St. Louis, Missouri; [4]Center for In Vivo Imaging and Therapeutics, St. Jude Children's Research Hospital, Memphis, Tennessee; and [5]Department of Biochemistry and Molecular Biophysics, Washington University School of Medicine, St. Louis, Missouri

Multiple myeloma (MM) is a plasma B-cell hematologic cancer that causes significant skeletal morbidity. Despite improvements in survival, heterogeneity in response remains a major challenge in MM. Cluster of differentiation 38 (CD38) is a type II transmembrane glycoprotein overexpressed in myeloma cells and is implicated in MM cell signaling. Daratumumab is a U.S. Food and Drug Administration–approved high-affinity monoclonal antibody targeting CD38 that is clinically benefiting refractory MM patients. Here, we evaluated [^{89}Zr]Zr-desferrioxamine (DFO)-daratumumab PET/CT imaging in MM tumor models. **Methods:** Daratumumab was conjugated to DFO-*p*-benzyl-isothiocyanate (DFO-Bz-NCS) for radiolabeling with ^{89}Zr. Chelator conjugation was confirmed by electrospray ionization-mass spectrometry, and radiolabeling was monitored by instant thin-layer chromatography. Daratumumab was conjugated to Cyanine5 (Cy5) dye for cell microscopy. In vitro and in vivo evaluation of [^{89}Zr]Zr-DFO-daratumumab was performed using CD38$^+$ human myeloma MM1.S-*luciferase* (MM1.S) cells. Cellular studies determined the affinity, immunoreactivity, and specificity of [^{89}Zr]Zr-DFO-daratumumab. A 5TGM1-*luciferase* (5TGM1)/KaLwRij MM mouse model served as control for imaging background noise. [^{89}Zr]Zr-DFO-daratumumab PET/CT small-animal imaging was performed in severe combined immunodeficient mice bearing solid and disseminated MM tumors. Tissue biodistribution (7 d after tracer administration, 1.11 MBq/animal, n = 4–6/group) was performed in wild-type and MM1.S tumor–bearing mice. **Results:** A specific activity of 55.5 MBq/nmol (0.37 MBq/μg) was reproducibly obtained with [^{89}Zr]Zr-daratumumab-DFO. Flow cytometry confirmed CD38 expression (>99%) on the surface of MM1.S cells. Confocal microscopy with daratumumab-Cy5 demonstrated specific cell binding. Dissociation constant, 3.3 nM (±0.58), and receptor density, 10.1 fmol/mg (±0.64), was obtained with a saturation binding assay. [^{89}Zr]Zr-DFO-daratumumab/PET demonstrated specificity and sensitivity for detecting CD38$^+$ myeloma tumors of variable sizes (8.5–128 mm^3) with standardized uptake values ranging from 2.1 to 9.3. Discrete medullar lesions, confirmed by bioluminescence images, were efficiently imaged with [^{89}Zr]Zr-DFO-daratumumab/PET. Biodistribution at 7 d after administration of [^{89}Zr]Zr-DFO-daratumumab showed prominent tumor uptake (27.7 ± 7.6 percentage injected dose per gram). In vivo blocking was achieved with a 200-fold excess of unlabeled daratumumab. **Conclusion:** [^{89}Zr]Zr-DFO- and Cy5-daratumumab demonstrated superb binding to CD38$^+$ human MM cells and significantly low binding to CD38^{low} cells. Daratumumab bioconjugates are being evaluated for image-guided delivery of therapeutic radionuclides.

Key Words: [^{89}Zr]Zr-DFO-daratumumab; cluster of differentiation 38 (CD38); multiple myeloma (MM); molecular imaging

J Nucl Med 2018; 59:216–222
DOI: 10.2967/jnumed.117.196063

Multiple myeloma (MM) is an age-related hematologic malignancy of antibody-secreting plasma B-cells with more than 30,000 new cases and 13,000 deaths in 2016 alone (*1*). MM remains an incurable disease, demonstrating a broad spectrum of aggression and resistance to treatment as a result of the genomic instability and clonal heterogeneity (*2*). The risk of skeletal-related events such as fractures is high in MM patients and continues to rise even with treatment (*3*). Advances in combination therapies, the advent of novel drugs such as proteasome inhibitors and immunomodulatory agents, and the success of stem cell transplantation have contributed to improvements in the 5-y survival rate in MM (*4*). However, the new therapies have not completely displaced the routine use of conventional chemotherapies, and the response is not uniform among MM patients. Therefore, there is an unmet need for innovative and personalized therapeutic approaches that will improve MM outcome, reduce toxicity, and induce long-term deep tumor regression. Recently treatment with monoclonal antibodies against antigens that are overexpressed in myeloma cells has demonstrated promising results (*5*). Antibodies are characterized by exquisite target specificity and are therefore ideal for targeting cell surface proteins that are selectively expressed on malignant cells (*6*). Also, because of high target affinity and specificity, antibodies can exert both cytotoxic and cytostatic properties by interfering with mechanisms involved in cell growth or signaling after binding to the target. For example, antibodies can induce tumor cell death through apoptosis or multiple immune-mediated mechanisms such as complement-dependent cytotoxicity, antibody-dependent cellular phagocytosis, and antibody-dependent cellular cytotoxicity.

All of these requirements are met by cluster of differentiation 38 (CD38) (*7*). CD38 is a single-chain type II transmembrane glycoprotein that has 256 amino acids in the extracellular domain, which act as an ectoenzyme, whereas the functional unit is a dimer

Received May 11, 2017; revision accepted Aug. 30, 2017.
For correspondence or reprints contact: Monica Shokeen, Department of Radiology, Mallinckrodt Institute of Radiology, 4515 McKinley Ave., 2nd Floor, St. Louis, MO 63110.
E-mail: mshokeen@wustl.edu
Published online Oct. 12, 2017.

with its central portion hosting the catalytic site (*8*). CD38 is expressed on terminally differentiated plasma cells as well as on the cell surface of lymphoid tumors such as MM, AIDS-associated lymphomas, and posttransplant lymphoproliferative disorders (*9*). The relatively high expression of CD38 on malignant plasma cells in combination with its role in modulating intracellular signaling make it an attractive therapeutic antibody target for treatment of MM (*10*).

Daratumumab is U.S. Food and Drug Administration–approved humanized IgG1 κ-monoclonal antibody that targets the CD38 epitope (*11*). Daratumumab binds to 2 β strands of CD38 containing amino acids 233–246 and 267–280 and is believed to demonstrate broad spectrum killing activity against CD38-expressing tumor cells by inducing tumor cell death through apoptosis and multiple immune-mediated mechanisms (*12*). Daratumumab has shown a favorable safety profile and encouraging efficacy in heavily pretreated relapsed and refractory MM patients, even as a single agent (*13*). However, not all of the heavily pretreated patients respond to single-agent daratumumab, and some patients who initially respond progress eventually (*14*). Therefore, there is a need for a companion diagnostic to stratify patients who will benefit from the daratumumab therapy. Antibody-based imaging agents are playing an ever more important role in the clinic as demonstrated by trastuzumab and pertuzumab bioconjugates for the human epidermal growth factor receptor 2 (HER2) imaging (*15*).

In this study, we evaluated daratumumab for PET/CT imaging of MM. The proof-of-principle in vitro and in vivo data in the $CD38^+$ human myeloma cells and MM mouse models demonstrated the potential of daratumumab-based imaging agents for stratifying patients for daratumumab therapy. Specific antibodies such as daratumumab are also attractive platforms for targeted α-particle radiation therapy (*16,17*).

We hypothesize that the enhanced specific expression of CD38 glycoprotein on malignant plasma cells will favor increased [^{89}Zr]Zr-desferrioxamine (DFO)-daratumumab uptake and allow for clinically impactful PET imaging for therapeutic planning as a companion diagnostic. The goal of this project was to develop and validate daratumumab-based imaging agents that will eventually help stratify patients for daratumumab therapy, minimizing off-target toxicities, and help reduce unnecessary treatment of patients not likely to respond. The safety profile and targeting efficacy of daratumumab render it an ideal candidate for radiation therapy as well in future studies. These studies will contribute toward technologic advancements in diagnostic and therapeutic monoclonal antibody–based radiopharmaceutical development for MM and lymphoid tumors in general.

MATERIALS AND METHODS

Ethics Statement

All experiments involving the use of radioactive materials at Washington University were conducted under the authorization of the Radiation Safety Commission in accordance with the University's Nuclear Regulatory commission license. All animal studies were performed under the guide for the Care and Use of Laboratory Animals under the auspices of the Washington University Animal Studies Committee. The data in any tables and any radiation or radiopharmaceutical doses mentioned are verified and correct.

All chemicals were purchased in the highest available purity, and solutions were prepared using ultrapure water (18 MΩ-cm resistivity; Millipore system). Daratumumab was provided by the Siteman Cancer Center pharmacy. DFO-Bz-NCS was purchased from Macrocyclics, Inc. The optical dye, Sulfo-Cyanine5 (Cy5) NHS ester, was purchased from Lumiprobe Corporation. All other chemicals used in the conjugation, radiolabeling, and purification steps were purchased from Sigma Aldrich. Electrospray ionization-mass spectrometry was performed using Thermo Exactive EMR (Thermo Fisher Scientific) at the Washington University Mass Spectrometry Core Facility. ^{89}Zr was produced via the ^{89}Y (p, n) ^{89}Zr reaction on a CS-15 cyclotron (Cyclotron Corp.) at Washington University Cyclotron Facility. The human MM cancer cell line MM1.S-Luciferase (MM1.S) was obtained from DiPersio Laboratory (Professor John F. DiPersio, Department of Medicine, Washington University School of Medicine). Murine MM cancer cell line (5TGM1-GFP) was obtained from Professor Katherine N. Weilbaecher (Department of Medicine, Oncology Division, Washington University School of Medicine). Achilefu Laboratory (Professor Samuel Achilefu, Department of Radiology, Washington University School of Medicine) developed the 5TGM1-GFP-luc (click beetle red luciferase) cell line.

Synthesis and Characterization of Daratumumab-DFO

For the synthesis of the daratumumab-DFO conjugate, daratumumab (20 mg/mL; 0.012 μmol) was incubated with DFO-Bz-NCS (0.18 μmol) using 0.1 M sodium carbonate (pH 9) as the conjugating buffer. The reaction mixture was incubated at 37°C for 1 h. Chelator was conjugated to the antibody via a thiourea linkage, and the conjugate was purified using Zeba spin columns (molecular weight cutoff = 40 kDa, 0.5 mL; Thermo Fisher Scientific). The protein concentration of resultant DFO functionalized antibody was determined by bicinchoninic acid assay (Thermo Fisher Scientific). Conjugation efficiency was evaluated by electrospray ionization-mass spectrometry.

Radiolabeling of Daratumumab-DFO with ^{89}Zr

Daratumumab-DFO conjugate was added to neutralized [^{89}Zr]Zr-oxalate, and the reaction mixture was incubated at 37°C for 1 h while being shaken. Radiochemical purity was determined by instant thin-layer chromatography using 50 mM diethylenetriaminepentaacetic acid as the mobile phase. The serum stability of the radiolabeled antibody was determined at 4 different time intervals (1, 2, 3, and 7 d).

Flow Cytometry, In Vitro Saturation Binding Assay, In Vitro Cell Uptake, and Immunoreactivity Assay

Details of flow cytometry, in vitro saturation binding assay, in vitro cell uptake, and immunoreactivity assay are provided upon request.

Synthesis of Daratumumab-Cy5

A freshly prepared 10-μL aliquot of Sulfo-Cyanine5 (Cy5) NHS ester (1 mg/mL in water) was added to 100 μL of daratumumab (20 mg/mL), and the total volume was adjusted to 200 μL using 0.1 M sodium carbonate buffer (pH 9). The Cy5 dye was added to daratumumab solution at a 5:1 molar ratio, and the reaction mixture was incubated at 37°C for 2 h with gentle shaking. Additional details about this synthesis are provided upon request.

Confocal Microscopy

MM1.S cells were plated on 35-mm glass bottom dishes coated with polylysine (MatTek Corp., glass no. 1.5) and incubated for an hour at 37°C, 5% CO_2 to let cells attach to the glass surface. To test binding to cell surface CD38, attached cells were treated with daratumumab-Cy5 (14 mg/mL, 1 μM with respect to Cy5) and Hoechst 33342 (10 μg/mL) for 10 min at 4°C with or without 100-fold molar excess of unlabeled daratumumab as a blocking agent. Additional details about this process are provided upon request.

Tissue Distribution of [^{89}Zr]Zr-Daratumumab in MM1.S Tumor–Bearing Mice

Tissue biodistribution studies were performed to evaluate the uptake of [^{89}Zr]Zr-DFO-daratumumab in normal (n = 4) and MM1.S

tumor–bearing severe combined immunodeficient (SCID) mice (n = 6). Bioluminsecence imaging was performed to confirm tumor location. Before tissue biodistribution studies, mice were injected via the lateral tail vein with 100 μL of 1.11 MBq of [^{89}Zr]Zr-DFO-daratumumab (specific activity, 55.5 MBq/nmol) in saline. Blocking studies were conducted with a 200-fold molar excess of cold daratumumab (100 μL) injected via the lateral tail vein at 15 min before the injection of [^{89}Zr]Zr-DFO-daratumumab (1.11 MBq) in mice. Additional details are provided upon request.

Small-Animal [^{89}Zr]Zr-Daratumumab PET/CT Imaging

Small-animal [^{89}Zr]Zr-DFO-daratumumab PET/CT imaging was conducted in Fox Chase severe combined immunodeficient (SCID) beige mice bearing MM1.S subcutaneous and disseminated myeloma tumors. Before small-animal PET/CT imaging, mice were injected via the lateral tail vein with [^{89}Zr]Zr-DFO-daratumumab (1.11 MBq). Additional details are provided upon request.

Data Analysis and Statistics

All data are presented as mean ± SD. Groups were compared using Prism 5.0 (GraphPad Software, Inc.). P values of less than 0.05 were considered statistically significant.

RESULTS

Synthesis and Characterization of Daratumumab-DFO

The anti-CD38 antibody, daratumumab, was modified with the bifunctional chelator DFO-Bz-NCS with a 15:1 molar excess of chelator to the antibody. On the basis of the electrospray ionization mass spectra, the calculated average number of chelators attached to a single antibody molecule was approximately 5–7.

Radiolabeling and Stability of Radiolabeled Daratumumab-DFO

Daratumumab-DFO was radiolabeled using neutralized [^{89}Zr]Zr-oxalate, resulting in the specific activity of 55.5 MBq/nmol. High radiochemical purity (>99%) was obtained after the labeled conjugate was purified using Zeba spin columns. The crude and purified compound was evaluated by radio thin-layer chromatography using 50 mM diethylenetriaminepentaacetic acid as the mobile phase. In vitro serum stability tests demonstrated that the radiolabeled antibody was stable with more than 98% intact radioactivity with the antibody for up to 7 d.

Flow Cytometry

For the proof-of-principle in vitro and in vivo studies, a CD38-expressing myeloma cell line was desirable. The human MM cell line MM1.S was derived from a biopsy sample from a 42-y-old African American woman and is commonly used for evaluating therapies in preclinical studies (*18*). Flow cytometry studies using MM1.S human myeloma cell line confirmed the high expression of CD38 antigen (>99% of cells staining positive) and therefore was used for cellular and in vivo studies (Fig. 1A). Flow cytometry additionally confirmed that the expression of CD38 on MM1.S cells remained intact after inoculation into SCID mice (Supplemental Fig. 1; supplemental materials are available at http://jnm.snmjournals.org).

In Vitro Saturation Binding, Cell Uptake, and Immunoreactivity Assay

[^{89}Zr]Zr-daratumumab demonstrated saturable binding to CD38$^+$ MM1.S human myeloma whole cells. The concentration at which the radiolabeled antibody occupied 50% of the cell surface receptors was determined to be 3.3 nM (±0.58). A representative saturation binding curve and Scatchard transformation of [^{89}Zr]Zr-DFO-daratumumab binding to MM1.S cells is shown in Fig. 1B. The data demonstrated that in the concentration range of 0.25–16.0 nM, [^{89}Zr]Zr-DFO-daratumumab is bound to a single class of binding sites with a receptor density of 10.1 fmol/mg (±0.64). Additionally, whole-cell uptake (sum of the cell internalized and cell surface bound fractions at 37°C) of [^{89}Zr]Zr-DFO-daratumumab in MM1.S cells in the presence and absence of the blocking agent (cold daratumumab) was significantly reduced ($P < 0.0001$) (Fig. 1C). The immunoreactive fraction determined using Lindmo assay was 95% (Supplemental Fig. 2).

Confocal Microscopy with Daratumumab-cy5

The sulfo-Cy5-NHS ester optical dye (5 equivalents) was successfully coupled to 1 equivalent of daratumumab, and the conjugates were characterized qualitatively by gel electrophoresis (data not shown). Gel electrophoresis results showed that the conjugation did not alter the fluorescence characteristics of the optical dye, and the excitation (646 nm) and emission (662 nm) spectra of the daratumumab-Cy5 conjugate were similar to that of free dye. The binding of daratumumab-Cy5 was evaluated in MM1.S cells using confocal microscopy. MM1.S cells were treated with daratumumab-Cy5 in the absence and presence of a 100-fold molar excess of unlabeled daratumumab. Confocal laser scanning microscopy images showed that MM1.S cells in the absence of block efficiently bound the fluorescent-antibody conjugate when compared with the cells in the presence of blocking, demonstrating the binding specificity of the conjugate (Fig. 2).

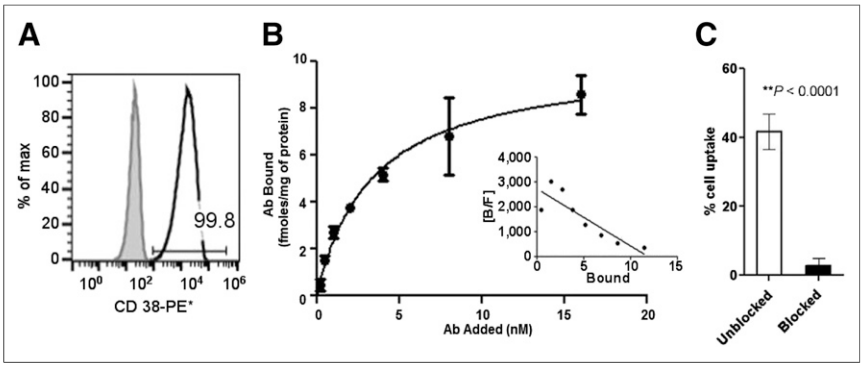

FIGURE 1. (A) Flow cytometry data validated >99% CD38$^+$ expression as compared with isotype control in human MM1.S myeloma cells. (B) Saturation binding curve for [^{89}Zr]Zr-DFO-daratumumab in MM1.S cells; n = 3. Inset shows Scatchard transformation of saturation binding data. (C) Percentage cell uptake of [^{89}Zr]Zr-DFO-daratumumab in MM1.S cells at 37°C in absence and presence of 100-fold blocking dose of cold daratumumab. PE = phycoerythrin.

Small-Animal PET/CT Imaging

Fox Chase SCID beige mice bearing MM1.S subcutaneous tumor xenografts when injected intravenously with [^{89}Zr]Zr-DFO-daratumumab demonstrated significant tumor-selective uptake. Small-animal PET images of these mice showed that the radiolabeled bioconjugate had appropriate sensitivity and selectivity for detecting myeloma tumors of different sizes and

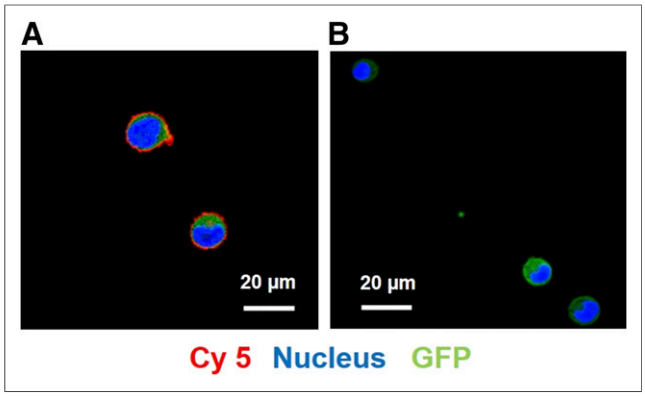

FIGURE 2. (A) Confocal microscopy images of MM1.S cells treated with daratumumab-Cy5 showed strong cell surface signal (red: Cy5, green: GFP, blue: Hoechst 33342 [nuclear costain]). (B) Cell surface binding is significantly reduced in presence of 100-fold molar excess of unlabeled anti-CD38 antibody as blocking agent. Scale bar represents 20 μm.

heterogeneity, as even early-stage nonpalpable, tumor lesions were clearly visible in the PET images (Fig. 3A). Region-of-interest analysis of PET images demonstrated that the SUVs ranged from 2.1 to 9.3 in tumors of different sizes and volumes (8.5–128 mm^3) (Figs. 3A and 3B). [^{89}Zr]Zr-DFO-daratumumab uptake was significantly reduced in the presence of a 200-fold molar excess of the cold antibody as shown in the PET image (Fig. 4A). The autoradiographic slices from excised tumors are in concert with the PET/CT imaging data, with reduced radioactivity in the blocked tumor (Fig. 4C). Representative bioluminescence and CT images of the mouse used in the blocking study confirmed the presence of tumor on the right flank (Figs. 4B and 4D). The CD38 expression is retained (>99%) in the engrafted MM1.S tumors as verified independently by flow cytometry (Supplemental Fig. 1). Daratumumab binds to human and chimpanzee CD38, but not to CD38 of other typical species used in preclinical research such as mouse, rat, rabbit, pig, and cynomolgus and rhesus monkey. For investigating the nonspecific retention due to the enhanced permeability and retention effect, we used the 5TGM1/KaLwRij intratibial tumor mouse model (Supplemental Fig. 3).

To demonstrate the in vivo imaging of skeletal tumor lesions, [^{89}Zr]Zr-DFO-daratumumab PET/CT was performed in a MM1.S disseminated MM mouse model (n = 4). The representative bioluminescence image (Fig. 5A) validated the tumor presence in the bone marrow–rich skeletal sites such as femur, tibia, and spinal cord. Mice with MM1.S-disseminated tumors were imaged at 7 d after administration of [^{89}Zr]Zr-DFO-daratumumab. The small-animal PET/CT images demonstrated significant radiotracer uptake in the tumor-bearing lesions. The representative images of the disseminated mouse model and the corresponding tumor-free SCID mouse are shown in Figure 5B.

Tissue Distribution of [^{89}Zr]Zr-DFO-Daratumumab in Wild-Type and Tumor-Bearing MM Mice

Tissue biodistribution studies were performed in the non-tumor and subcutaneous MM1.S tumor–bearing SCID mice, respectively, using [^{89}Zr]Zr-DFO-daratumumab at 6 and 7 d after administration of the radiopharmaceutical. Biodistribution studies in a disseminated tumor model are challenging as the bones are rendered fragile because of myeloma-induced lysis. The biodistribution data in the subcutaneous tumor mice were in agreement with the PET imaging data showing considerably high uptake and retention in tumor tissue at 7 d after injection with the uptake of 27.7 ± 7.6 percentage injected dose per gram (%ID/g) (Fig. 6). A high concentration of radioactivity was seen in the spleen with 31.5 ± 7.5 %ID/g, as previously observed with [^{89}Zr]Zr-DFO-labeled antibodies in vivo (*19,20*). The %ID/g in remaining normal tissues was significantly lower than in the tumor tissues. The [^{89}Zr]Zr-DFO-daratumumab tissue biodistribution in nontumor-SCID mice showed the expected trend with the highest %ID/g retention in the spleen (25.6 ± 3.4) (Supplemental Table 1).

A separate set of mice was used to perform blocking studies to evaluate the specificity of [^{89}Zr]Zr-DFO-daratumumab in vivo in the MM1.S xenograft subcutaneous mouse model. In the blocking group, splenic uptake (31.5 ± 6.1 vs. 10.6 ± 1.4) and tumor-associated activity was significantly reduced (~3-fold decrease) when compared with the nonblocked tumor. The blocking study did not significantly alter the uptake in other nontumor tissues (Supplemental Table 2).

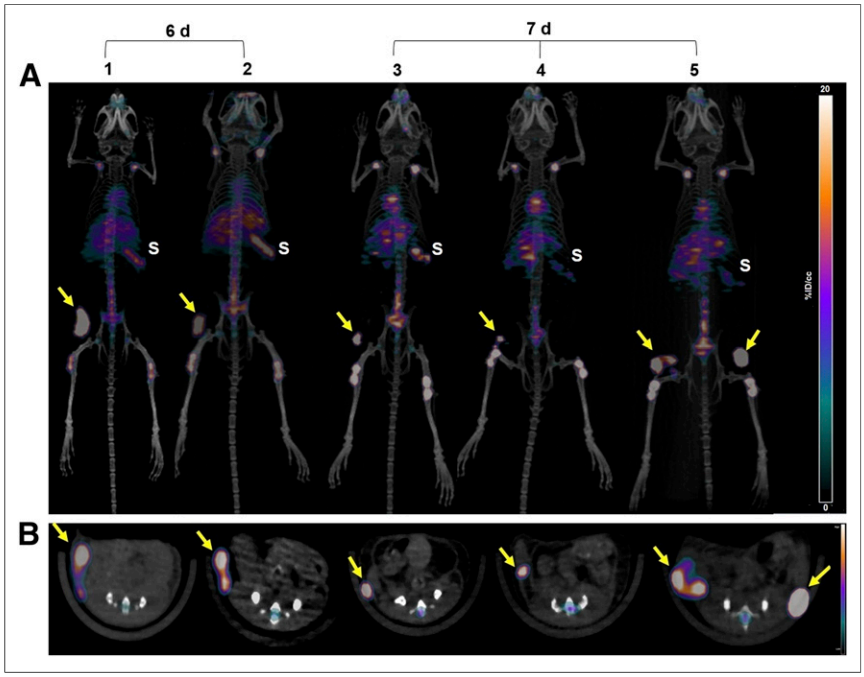

FIGURE 3. (A) Representative maximum-intensity-projection coronal [^{89}Zr]Zr-DFO-daratumumab PET/CT images in MM1.S subcutaneous tumor–bearing SCID mice at 6 d (n = 2) and 7 d (n = 3) after injection of radiopharmaceutical. (B) Axial planes corresponding to images shown in A. Nonpalpable and palpable tumors with volumes ranging from 8.47 to 128.1 mm^3 showed efficient tracer uptake. S = spleen; tumors = yellow arrows.

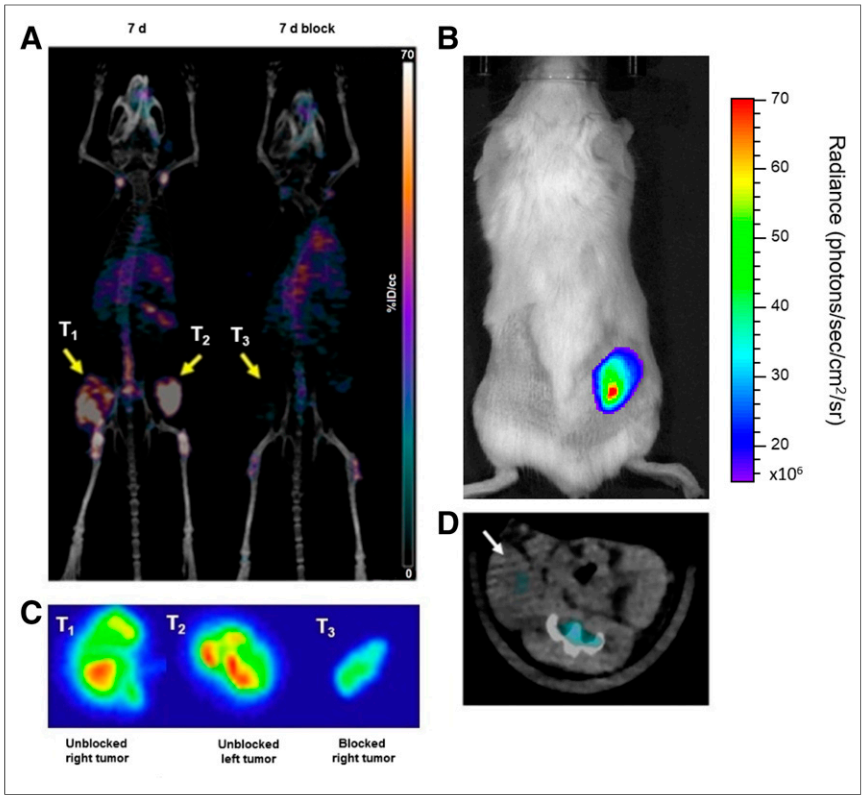

FIGURE 4. (A; left) Representative maximum-intensity-projections [^{89}Zr]Zr-DFO-daratumumab/PET/CT image of mouse with bilateral subcutaneous MM1.S tumors (T_1 and T_2) in absence of blocking agent. (A; right) [^{89}Zr]Zr-DFO-daratumumab/PET/CT image of mouse with unilateral subcutaneous MM1.S tumor (T_3) that received 200-fold molar excess of cold daratumumab as blocking agent. Both mice were imaged at 7 d after injection of [^{89}Zr]Zr-DFO-daratumumab. (B) Representative bioluminescence image of subcutaneous MM1.S tumor (T_3)–bearing mouse used for blocking study. (C) Representative autoradiography images of frozen tumor slices showing distribution of [^{89}Zr]Zr-DFO-daratumumab within imaged MM1.S tumors (T_1, T_2, T_3). (D) Axial CT image of mouse used in blocking study. Subcutaneous tumor (white arrow) is confirmed in bioluminescence image.

DISCUSSION

High expression of CD38 antigen on malignant plasma cells complemented with a relatively low expression on normal lymphoid and myeloid cells make it a desirable therapeutic target (*10*). Approved by the U.S. Food and Drug Administration in 2016, daratumumab is a therapeutic human monoclonal antibody with high affinity for the unique CD38 epitope. Daratumumab has demonstrated a favorable safety profile and efficacy as monotherapy and in combination with other drugs in pretreated relapsed and refractory myeloma patients (*13*). Preclinical studies published by de Weers et al. suggested that daratumumab effectively killed primary CD38$^+$ and CD138$^+$ patient MM cells and a range of MM cell lines by antibody-dependent cellular and complement-dependent cytotoxicity mechanisms (*15*). Although promising clinically, not all patients respond to daratumumab monotherapy, highlighting the need for patient stratification for daratumumab therapy. Additionally, an effective strategy to identify responsive from nonresponsive phenotypes will help us to understand the mechanisms of resistance and eventually lead to methods for overcoming resistance through sensitization to therapy.

Antibodies have evolved as reliable vehicles for the delivery of radionuclides and drugs to cancer cells due to their high selectivity and affinity. Radiolabeled antibody–based agents directed toward tumor-associated antigens can be used to evaluate the specific uptake by cancer molecular biomarkers. Antibody-based imaging agents are making a positive impact in the clinic by helping to stratify patients for targeted therapies and monitoring therapy responses based on the level of tumor-associated antigen expression (*21–23*).

^{89}Zr is a desirable and validated long-lived PET radionuclide with a half-life of 3.3 d that matches the slow pharmacokinetics of the intact antibodies (*24*). The DFO ligand coordinates Zr^{4+} easily at room temperature and is stable in human serum for up to 7 d, and [^{89}Zr]Zr-DFO–based PET images have demonstrated excellent spatial resolution and signal-to-noise ratios in human patients (*15*). Human radiation dosimetry of [^{89}Zr]Zr-DFO-trastuzumab in patients with HER2-positive breast cancer showed that it is safe for human applications (*25,26*). There are currently over 20 ongoing clinical trials to evaluate antibody-based imaging agents for imaging and treating different solid and hematologic cancers (*27*). Moreover, these clinical studies are geared to image the expression of proteins that would benefit from targeted therapy, evaluate treatment response, and detect recurrent cancers (*28*).

A sensitive, noninvasive functional PET imaging probe is highly desirable to evaluate the expression of CD38 in myeloma cells for therapy planning of MM patients. Targeted molecular imaging approaches could also help in differentiating MM from other monoclonal plasma cell malignancies (*29,30*). Therefore, we evaluated the efficacy of [^{89}Zr]Zr-DFO-daratumumab to image CD38$^+$ expression in mouse models of MM. We demonstrated that DFO-daratumumab could be stably and reproducibly labeled with ^{89}Zr while preserving the antigen binding capacity. CD38$^+$ click beetle red–transfected MM1.S human myeloma cells were used for in vitro and in vivo proof-of-principle studies for evaluating [^{89}Zr]Zr-DFO-daratumumab. [^{89}Zr]Zr-DFO-daratumumab demonstrated high affinity for the human myeloma cell line MM1.S in vitro and in vivo. Flow cytometry and cell uptake assays confirmed the high expression of CD38 on MM1.S cells in vitro and ex vivo. The cell uptake and saturation binding assays showed that [^{89}Zr]Zr-DFO-daratumumab can bind with high affinity and specificity to CD38$^+$ myeloma cells. Importantly, the immunoreactivity of [^{89}Zr]Zr-DFO-daratumumab was determined to be more than 95%.

Preclinical PET/CT imaging with [^{89}Zr]Zr-DFO-daratumumab was supported by in vitro cell binding and uptake studies, fluorescence confocal microscopy, ex vivo biodistribution, and autoradiography of the tumor slices. Ex vivo tissue biodistribution data demonstrated that [^{89}Zr]Zr-DFO-daratumumab had specific uptake in MM1.S myeloma tumors at 6 and 7 d after administration of the radiopharmaceutical. The tumor uptake was considerably reduced in the presence of excess unlabeled daratumumab, demonstrating

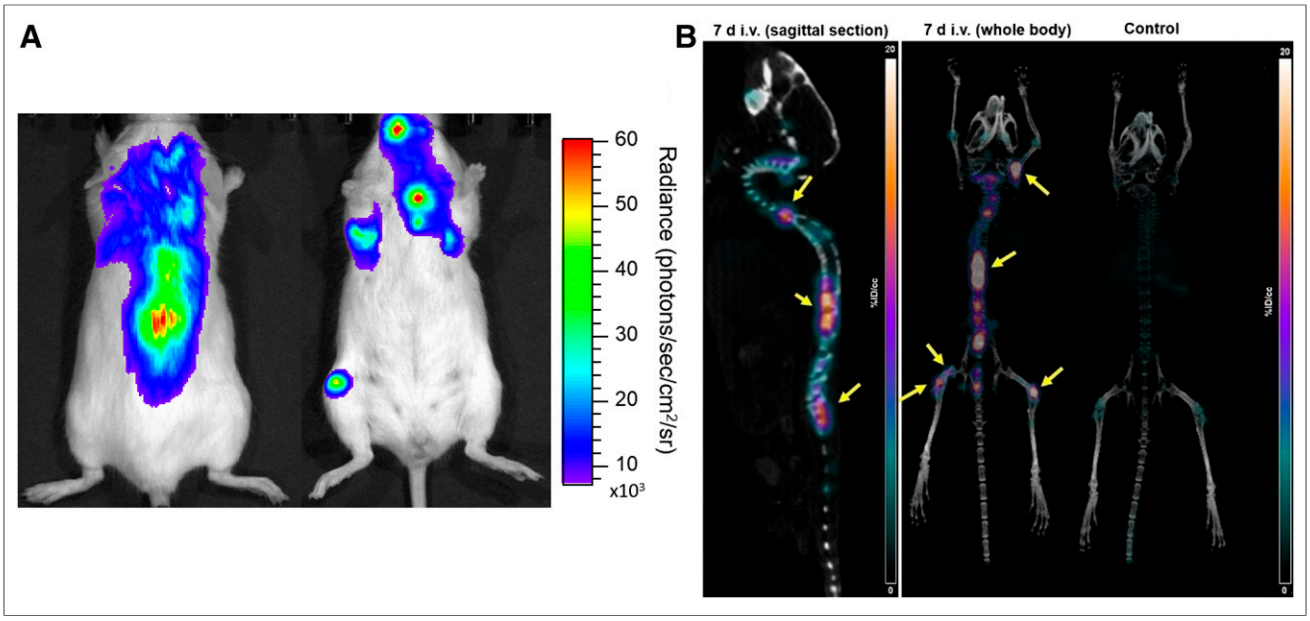

FIGURE 5. (A) Representative bioluminescence image of mouse in prone and supine positions demonstrating extent of tumor progression in disseminated MM1.S tumor model. (B) [^{89}Zr]Zr-DFO-daratumumab PET/CT image (sagittal and coronal views) of disseminated MM1.S tumor–bearing mouse and nontumor control mouse.

specificity and affinity of the monoclonal antibody for CD38^{+} cells in vivo.

PET imaging performed at 6 and 7 d after administration of [^{89}Zr]Zr-DFO-daratumumab in mice bearing subcutaneous MM tumors showed high radiotracer uptake in tumors of variable sizes with a superb tumor-to-background contrast. Furthermore, PET images in the disseminated mouse model showed that the tumor cells localized in femur, tibia, and spine were readily detectable by [^{89}Zr]Zr-DFO-daratumumab. The enhanced permeability and retention effect did not significantly contribute toward [^{89}Zr]Zr-DFO-daratumumab signal in tumor lesions. As previously shown in mice, relatively high uptake occurred in the spleen and bone. In organs such as the spleen, blood capillaries have sinusoidal clefts of about 100 nm allowing monoclonal antibodies to freely travel through these clefts, partly explaining the splenic uptake (*31*). Previous studies have shown elevated levels of ^{89}Zr in the remodeling bones of mice injected with [^{89}Zr]Zr-DFO-labeled antibodies, attributed to metabolism of osteophilic ^{89}Zr^{4+} from the ligand in vivo by less selective mouse liver enzymes (*32,33*). Human studies with [^{89}Zr]Zr-DFO–labeled antibodies have, however, shown minimal uptake in bone (*34*). Thus, our preclinical data demonstrate that [^{89}Zr]Zr-DFO-daratumumab is a promising antibody-based PET radiopharmaceutical for noninvasive imaging of CD38^{+} myeloma tumors.

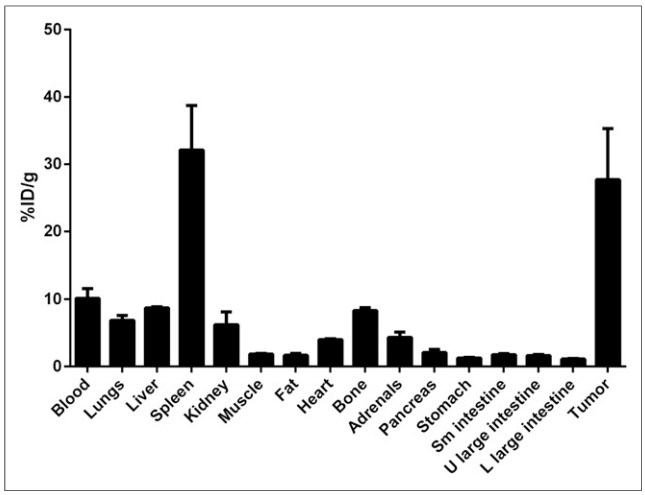

FIGURE 6. Biodistribution of [^{89}Zr]Zr-DFO-dararumumab in human MM1.S subcutaneous xenografts (n = 3) at 7 d after administration of radiotracer. L = lower; U = upper.

CONCLUSION

We have developed daratumumab-based PET and optical imaging probes that specifically target CD38 antigen and can be used to image CD38^{+} tumors with high specificity. These studies demonstrate the potential of [^{89}Zr]Zr-DFO-daratumumab as a PET molecular imaging agent for MM for diagnosis, patient stratification, and long-term follow-up.

DISCLOSURE

This research was primarily funded by the R01 CA176221 and U54 CA199092. We acknowledge the support from P50 CA094056, P30 CA091842, DE-SC0012737 and the MIR pilot imaging funds (17-016). No other potential conflict of interest relevant to this article was reported.

ACKNOWLEDGMENTS

Gail Sudlow assisted in intravenous injections. We are grateful to Dr. Richard Wahl for insightful comments. Special thanks go to

Dr. Bernadette Marquez and Deep Hathi for training and assisting Dr. Ghai.

REFERENCES

1. Kuehl WM, Bergsagel PL. Multiple myeloma: evolving genetic events and host interactions. *Nat Rev Cancer.* 2002;2:175–187.
2. Kuehl WM, Bergsagel PL. Molecular pathogenesis of multiple myeloma and its premalignant precursor. *J Clin Invest.* 2012;122:3456–3463.
3. Kyle RA, Gertz MA, Witzig TE, et al. Review of 1027 patients with newly diagnosed multiple myeloma. *Mayo Clin Proc.* 2003;78:21–33.
4. Kumar SK, Rajkumar SV, Dispenzieri A, et al. Improved survival in multiple myeloma and the impact of novel therapies. *Blood.* 2008;111:2516–2520.
5. Tai YT, Anderson KC. Antibody-based therapies in multiple myeloma. *Bone Marrow Res.* 2011;2011:924058.
6. Parren PW, van de Winkel JG. An integrated science-based approach to drug development. *Curr Opin Immunol.* 2008;20:426–430.
7. Malavasi F, Deaglio S, Damle R, et al. CD38 and chronic lymphocytic leukemia: a decade later. *Blood.* 2011;118:3470–3478.
8. Deaglio S, Mehta K, Malavasi F. Human CD38: a (r)evolutionary story of enzymes and receptors. *Leuk Res.* 2001;25:1–12.
9. van de Donk NW, Janmaat ML, Mutis T, et al. Monoclonal antibodies targeting CD 38 in hematological malignancies and beyond. *Immunol Rev.* 2016;270:95–112.
10. Stevenson GT. CD 38 as a therapeutic target. *Mol Med.* 2006;12:345–346.
11. McKeage K. Daratumumab: first global approval. *Drugs.* 2016;76:275–281.
12. de Weers M, Tai YT, van der Veer MS, et al. Daratumumab, a novel therapeutic human CD38 monoclonal antibody, induces killing of multiple myeloma and other hematological tumors. *J Immunol.* 2011;186:1840–1848.
13. Phipps C, Chen Y, Gopalakrishnan S, et al. Daratumumab and its potential in the treatment of multiple myeloma: overview of the preclinical and clinical development. *Ther Adv Hematol.* 2015;6:120–127.
14. Nijhof IS, Casneuf T, van Velzen J, et al. CD38 expression and complement inhibitors affect response and resistance to daratumumab therapy in myeloma. *Blood.* 2016;128:959–970.
15. Wang RE, Zhang Y, Tian L, et al. Antibody-based imaging of HER-2: moving into the clinic. *Curr Mol Med.* 2013;13:1523–1537.
16. Maguire WF, McDevitt MR, Smith-Jones PM, et al. Efficient 1-step radiolabeling of monoclonal antibodies to high specific activity with Ac-225 for α-particle radioimmunotherapy of cancer. *J Nucl Med.* 2014;55:1492–1498.
17. Jurcic JG, Larson SM, Sgouros G, et al. Targeted at particle immunotherapy for myeloid leukemia. *Blood.* 2002;100:1233–1239.
18. Greenstein S, Krett NL, Kurosawa Y, et al. Characterization of the MM.1 human multiple myeloma (MM) cell lines: a model system to elucidate the characteristics, behavior, and signaling of steroid-sensitive and -resistant MM cells. *Exp Hematol.* 2003;31:271–282.
19. Nagengast WB, de Vries EG, Hospers GA, et al. In vivo VEGF imaging with radiolabeled bevacizumab in a human ovarian tumor xenograft. *J Nucl Med.* 2007;48:1313–1319.
20. Marquez BV, Ikotun OF, Zheleznyak A, et al. Evaluation of ^{89}Zr-pertuzumab in breast cancer xenografts. *Mol Pharm.* 2014;11:3988–3995.
21. van de Watering FC, Perk L, Brinkmann U, et al. Zirconium-89 labeled antibodies: a new tool for molecular imaging in cancer patients. *BioMed Res Int.* 2014;2014:203601.
22. Muselaers CH, Stillebroer AB, Desar IM, et al. Tyrosine kinase inhibitor sorafenib decreases ^{111}In-girentuximab uptake in patients with clear cell renal cell carcinoma. *J Nucl Med.* 2014;55:242–247.
23. van Dongen GA, Visser GW, Lub-de Hooge MN, et al. Immuno-PET: a navigator in monoclonal antibody development and applications. *Oncologist.* 2007;12:1379–1389.
24. Zeglis BM, Lewis JS. The bioconjugation and radiosynthesis of ^{89}Zr-DFO-labeled antibodies. *J Vis Exp.* 2015;96:e52521.
25. Laforest R, Lapi SE, Oyama R, et al. [^{89}Zr]trastuzumab: evaluation of radiation dosimetry, safety, and optimal imaging parameters in women with HER2-positive breast cancer. *Mol Imaging Biol.* 2016;18:952–959.
26. Börjesson PK, Jauw YW, de Bree R, et al. Radiation dosimetry of ^{89}Zr-labeled chimeric monoclonal antibody U36 as used for immuno-PET in head and neck cancer patients. *J Nucl Med.* 2009;50:1828–1836.
27. Sliwkowski MX, Mellman I. Antibody therapeutics in cancer. *Science.* 2013;341:1192–1198.
28. Warram JM, de Boer E, Sorace AG, et al. Antibody-based imaging strategies for cancer. *Cancer Metastasis Rev.* 2014;33:809–822.
29. Vij R, Fowler KJ, Shokeen M. New approaches to molecular imaging of multiple myeloma. *J Nucl Med.* 2016;57:1–4.
30. Lemaire M, D'Huyvetter M, Lahoutte T, et al. Imaging and radioimmunotherapy of multiple myeloma with anti-idiotypic Nanobodies. *Leukemia.* 2014;28:444–447.
31. Tabrizi M, Bornstein GG, Suria H. Biodistribution mechanisms of therapeutic monoclonal antibodies in health and disease. *AAPS J.* 2010;12:33–43.
32. Abou DS. *In vivo* biodistribution and accumulation of ^{89}Zr in mice. *Nucl Med Biol.* 2011;38:675–681.
33. Terwisscha van Scheltinga AG, Ogasawara A, Pacheco G, et al. Preclinical efficacy of an antibody-drug conjugate targeting mesothelin correlates with quantitative ^{89}Zr-ImmunoPET. *Mol Cancer Ther.* 2017;16:134–142.
34. Dijkers EC, Oude Munnink TH, Kosterink JG, et al. Biodistribution of ^{89}Zr-trastuzumab and PET imaging of HER2-positive lesions in patients with metastatic breast cancer. *Clin Pharmacol Ther.* 2010;87:586–592.